Farnesene and norbornenyl methacrylate block copolymers: application of thiol-ene clicking to improve thermal and mechanical properties

Sharmaine B. Luk, Milan Maric*

McGill University, Department of Chemical Engineering, 3610 Rue University Rm 3060, Montréal, Canada, H3A 0C5

Corresponding author is at McGill University, Department of Chemical Engineering, 3610 Rue University Rm 3060, Montréal, Canada, H3A 0C5. Email address: milan.maric@mcgill.ca

Abstract

Novel block copolymers were synthesized for the first time via nitroxide-mediated polymerization (NMP) using ethylene glycol dicylopentenyl methacrylate (EGDEMA), which has a pendent double bond in the norbornene group, and farnesene (Far), a terpene-based diene. Homo poly(EGDEMA)) was synthesized successfully using Dispolreg 007 initiator without any co-monomer as typically required of NMP, and the macroinitiator was chain-extended with Far making poly(EGDEMA-*b*-Far) diblock copolymers. Due to the relatively low glass transition temperature (T_g) of poly(EGDEMA), the methacrylate block was also copolymerized statistically with isobornyl methacrylate (iBOMA) to add stiffness, then chain-extended with Far. Additionally, the pendent double bond of EGDEMA allowed for thiol-ene clicking of POSS units for further functionalization of these block copolymers. However, the conjugation efficiency of the thermally initiated thiol-ene clicking was low and resulted in low POSS incorporation (1.6 – 10 mol%), especially for block copolymers that included iBOMA due to its increased stiffness and steric hindrance. Nonetheless, the added POSS improved the thermal stability by minimizing the degradation of the 1,4-addition Far units, as well as the degradation of isobornyl units of iBOMA. The mechanical strength was also increased as POSS units reinforced the physical crosslinks of these block copolymers as shown by an increase in linear viscoelastic regions. Distinct T_gs were observed for the respective elastomeric poly(Far) block (~-70°C) and thermoplastic block (30°C for poly(EGDEMA) and 110°C for poly(EGDEMA-*co*-iBOMA)), therefore suggesting microphase separation. An increase in T_g was also observed in all polymers with added POSS, further confirming the added stiffness provided by POSS. These poly(EGDEMA-*b*-Far) and poly(EGDEMA-*co*-iBOMA-*b*-Far) show great versatility as alternative TPE materials, with improved mechanical and thermal properties added by functionalization of POSS.

Keywords

Block copolymers, thermoplastic elastomers, thiol-ene clicking, POSS

1 Introduction

Thermoplastic elastomers (TPEs) are very industrially relevant as they exhibit rubbery properties at usage temperatures but can still be processed at high temperatures like thermoplastics. Unlike vulcanized or chemically crosslinked elastomers (i.e. thermosets), TPEs are made of hard thermoplastics with high glass transition temperatures (T_g above ambient temperature) that act as physical crosslinks and soft elastomers serving as a matrix with low T_g [1]. Due to the immiscibility of the respective polymers, these polymers undergo phase separation, which is important for providing mechanical strength in the material. Some TPEs are made of a blend of polymers that are melt-mixed and cured to ensure interfacial bonding, such as ethylene-propylene rubber and polypropylene (PP), ethylene-propylene-diene terpolymer and PP, or poly(styrene-*b*-(ethylene-*co*-butadiene)-*b*-styrene) (SEBS) and PP [2-4]. In the latter case, SEBS itself is a TPE being a block copolymer that is a partially hydrogenated version of poly(styrene-*b*-butadiene-*b*-styrene) (SBS) [5, 6]. Block or grafted copolymers differ from melt-blended copolymers as they are synthesized by more sophisticated methods like living polymerization and therefore do not require post-polymerization blending [7]. Furthermore, melt-blended polymers exhibit macrophase separation, as opposed to block copolymers which exhibit microphase separation and can lead to various morphologies of the dispersed domains such as spheres, cylinders, or lamellae [1].

As mentioned, SBS and SEBS are typically synthesized via living polymerization. Living, or more specifically, ionic polymerization applies the ionic nature of the active polymerization site and can produce polymers with precise molecular architecture, like block copolymers, with low dispersity [8, 9]. However, this method requires stringent conditions (i.e. no impurities, absence of water) and is intolerant to functional monomers, thereby necessitating the use of protecting groups in some cases. Reversible deactivation radical polymerization (RDRP) employs the simplicity of radical polymerization, but it is also able to make block copolymers with low dispersity via the persistent radical effect (PRE) or reversible chain transfer [10]. In this method, the active polymerization site is a radical that is suppressed with a radical deactivator or chain transfer agent in an equilibrium such that irreversible termination is suppressed. In addition, RDRP is able to polymerize a wide variety of functional monomers derived from (meth)acrylates, styrenics, and (meth)acrylamides, not only in bulk or solution, but in aqueous dispersions, as well [11].

There are three main types of RDRP: nitroxide-mediated polymerization (NMP), atom transfer radical polymerization (ATRP), and reversible addition-fragmentation transfer (RAFT) polymerization. ATRP uses a metallic catalyst that reversibly abstracts a halogen atom which allows for polymerization to occur and it is suited for many monomers except for dienes [12]. It was not until very recently that copper-mediated ATRP with the proper ligands and conditions proved to be successful for polymerization of butadiene and isoprene [13, 14]. RAFT typically uses a dithioester chain transfer agent to control the polymerization of many monomers including dienes, vinyl esters, and methacrylates [15, 16]. NMP uses a nitroxide to deactivate the radical active centre in polymerization [17]. It was first used to polymerize styrene and then successfully used to synthesize SBS and demonstrated that NMP was a viable alternative to ionic polymerization to produce TPEs [18].

Common TPEs are made of poly(olefins) as one of the block components, which are byproducts of crude oil. Recently, it has become apparent that movement towards bio-sourced materials is important towards lessening the impact on the environment, among other initiatives. Myrcene is a terpene-based diene that is formed from the pyrolysis of β-pinene, which is found in tree sap [19, 20]. Farnesene is a similar monomer that is derived from terpenoids but can be produced by microorganisms [21-23]. Myrcene and farnesene are bio-based alternatives to petroleum-derived butadiene or isoprene and have been successfully polymerized ionically or using RDRP to make rubbery materials similar to poly(butadiene) and poly(isoprene) [24-28]. They also have low T_gs (T_g ~ -70°C for both poly(myrcene) and poly(farnesene), similar to T_g = -100°C for poly(butadiene)) with the potential of improved viscoelastic properties due to their bottlebrush-like structure from the long side-chains making them good candidates for TPEs [29, 30]. However, poly(myrcene) (M_e = 17,000 g mol^{-1}) and poly(farnesene) (M_e = 50,000 g mol^{-1}) have higher entanglement molecular weights due to their longer side chains relative to poly(butadiene) (M_e = 2,000 g mol^{-1}) [31].

Farnesene (Far) has been polymerized via NMP using SG1-based BlocBuilder and Dispolreg 007 initiators, and copolymerized with other functionalized methacrylates such as glycidyl methacrylate and isobornyl methacrylate (iBOMA) [32, 33]. Similarly, myrcene has been polymerized with NMP and block copolymers made with myrcene and iBOMA showed increased thermal stability and mechanical properties, which suggests that polymers synthesized with bio-based dienes and functionalized methacrylates have potential to be effective, versatile TPEs [34]. One such methacrylic co-monomer that has not been widely studied interest is ethylene glycol

dicyclopentenyl ether methacrylate (EGDEMA), which contains a norbornene group with a pendent double bond, in addition to the methacrylate. The polymerization of EGDEMA was previously reported for NMP, however using the conventional SG1-based initiator led to high dispersity (Đ ~ 1.56 – 1.74) and irreversibly terminated polymer chains without copolymerizing with styrene comonomer [35]. SG1-based initiators often require controlling comonomer when polymerizing methacrylates due to slow deactivation between the radical centre and nitroxide [36-38]. Consequently, Dispolreg 007 (D7) initiator was developed to be able to homopolymerize methacrylates with active chain-ends and does not require controlling comonomer [39, 40].

Poly(EGDEMA) was shown to be resistant to bacterial attachment and therefore used in many anti-bacterial films and coatings applications [41-43]. However, poly(EGDEMA) has a relatively low T_g (28°C) compared to other poly(methacrylates) like isobornyl methacrylate (iBOMA), which also contains a norbornyl group and has a very high T_g (up to 190°C), and the latter is bio-sourced as well [44, 45]. The reason EGDEMA has a low T_g, unlike iBOMA, is due to the chain mobility provided by the ethylene glycol ether bonds, whereas the bond attaching the norbornyl group to the methacrylate in iBOMA is much more rigid. Poly(EGDEMA) homopolymer and triblock copolymers were successfully synthesized by ATRP and have been shown to undergo post-polymerization thiol-ene clicking chemistry with thiol-containing molecules [44, 46].

In this study, the synthesis of poly(EGDEMA-*b*-Far) diblock copolymers by NMP was investigated using D7 initiator for the first time. Thiol-ene clicking was done on the resulting block copolymers with a thiol-containing polyhedral oligomeric silsesquioxanes (thiol-POSS) (Schematic 1) to modify the properties of the soft polydiene. POSS is a bulky inorganic-organic cage-like molecule made of Si_8O_{12} and alkyl substituents and has been copolymerized or used as an additive to improve mechanical properties, thermal stability, and anti-flammability in polymer materials [47-50]. Furthermore, POSS has been successfully clicked onto azido-functionalized SEBS, reinforcing the thermoplastic elastomer [51]. The EGDEMA methacrylate block was also copolymerized with iBOMA, then chain-extended with Far to increase the T_g of the methacrylate block, in addition to thiol-ene clicking with thiol functionalized POSS. The thermal properties and rheology of the block copolymers were studied to compare between different concentrations of thiol-POSS added, block copolymer compositions, and with and without copolymerization with iBOMA. The aim of this study is to show these poly(methacrylate-*b*-farnesene) block copolymers with the addition of POSS groups could potentially be an alternative TPE with improved thermal properties.

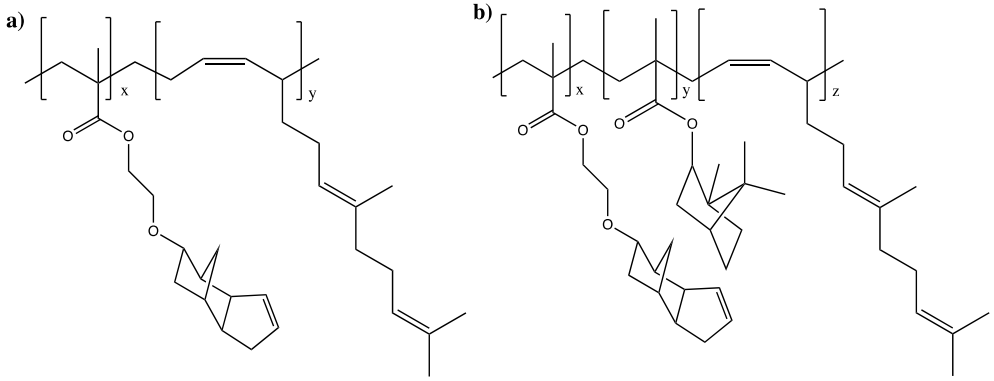

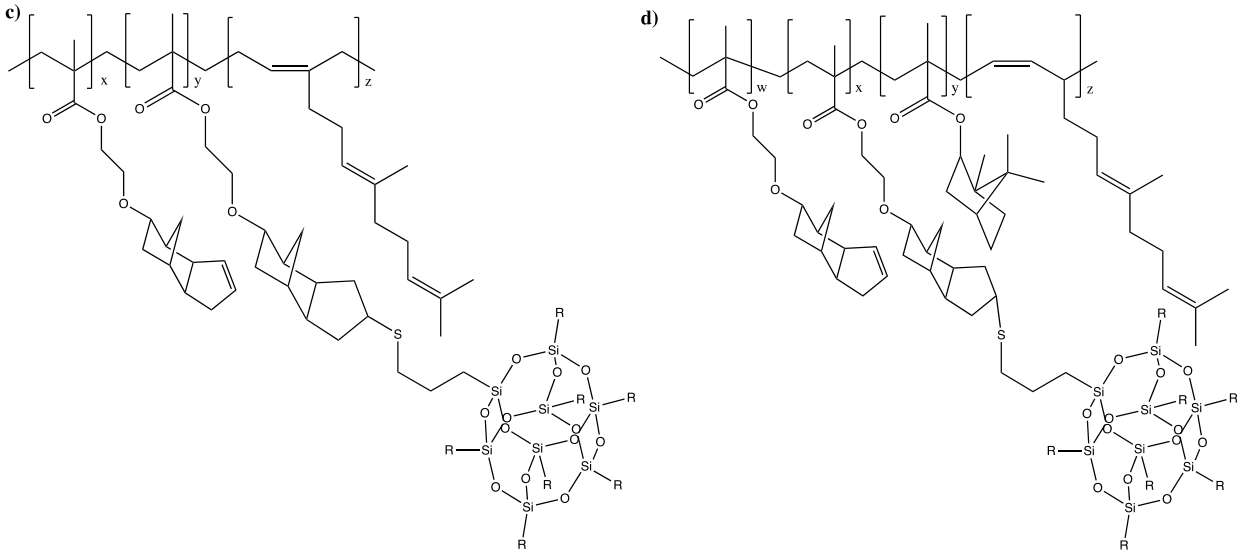

Schematic 1: Chemical structures of a) poly(EGDEMA-b-Far) and b) poly(EGDEMA-co-iBOMA-b-Far) block copolymers synthesized via NMP using D7 initiators. These block copolymers then underwent thiol-ene clicking with thiol-POSS and the proposed chemical structures are shown in c) and d). The R groups on the POSS units represent isobutyl groups.

2 Experimental Methods

2.1 Materials

Ethylene glycol dicyclopentenyl ether methacrylate (EGDEMA ≥ 90%) was purchased from Millipore Sigma. Isobornyl methacrylate (VISIOMER®, Terra iBOMA) monomer was obtained from Evonik. Trans-β-farnesene, or Biofene (Far ≥ 95%), was obtained from Amyris. Monomers were purified using 1.0 g of aluminum oxide (basic Al_2O_3, activated, Brockmann I) and 0.05 g calcium hydride (CaH_2, ≥90%) per 50 mL of monomer, which were used as purchased from Millipore Sigma. Mercaptopropyl isobutyl polyhedral oligomeric silsesquioxanes (thiol-POSS, 100%) was purchased from Hybrid Plastics Inc, and used as received. Azobisisobutyronitrile (AIBN, 98%) radical initiator was used as received from Millipore Sigma. Toluene (≥ 99.5%), xylene (≥ 98.5%), methanol (MeOH, ≥ 99.8%), and tetrahydrofuran (THF, 99.9% HPLC grade) were purchased from Fisher Chemicals and used as received. Deuterated chloroform ($CDCl_3$, 99.9% D) was purchased from Cambridge Isotope Laboratories, USA and used as received. Dispolreg 007 initiator was synthesized according to the procedure described by Ballard *et al* [39].

2.2 Synthesis of poly(EGDEMA) or poly(EGDEMA-co-iBOMA) macroinitiator

A typical formulation for the synthesis of poly(EGDEMA) macroinitiator was 0.3 g (0.89 mmol) of D7, 8.86 g (33.8 mmol) of EGDEMA monomer, and 8.86 g (96.2 mmol) of toluene solvent added into a 50 mL three-neck round bottom flask. The reactor was attached to a condenser to prevent evaporation of solvent and monomer. For the poly(EGDEMA-*co*-iBOMA) macroinitiators, 0.30 g of D7 was added, along with an equimolar mixture of EGDEMA (4.07 g, 18.3 mmol) and iBOMA (4.80 g, 18.3 mmol) monomers and 8.86 g (96.2 mmol) of toluene.

Detailed formulations for macroinitiator synthesis are shown in Table 1. The mixture was then purged with nitrogen for 30 mins and reaction would proceed under nitrogen atmosphere at 90°C with stirring. The reaction time would vary between 60 to 120 min depending on the desired chain length for the macroinitiators. The resulting polymers were precipitated with methanol, then dried under air overnight and in a vacuum oven at room temperature for a day, and they are characterized in Table 1.

Table 1: Formulations for poly(EGDEMA) and poly(EGDEMA-co-iBOMA) macroinitiator synthesis at 90°C and polymer characterization.

Macroinitiator ID	m_{D7} (g mL^{-1})	m_{EGDEMA} (g mL^{-1})	m_{iBOMA} (g mL^{-1})	$m_{toluene}$ (g mL^{-1})	X	M_n of macroinitiator (g mol^{-1})	Đ	F_{EGDEMA}	F_{iBOMA}
EG1	0.0161	0.477	-	0.477	32.0%	7,500	1.57	1.00	-
EG2	0.00538	0.477	-	0.477	46.7%	15,700	1.64	1.00	-
EGiB1	0.0158	0.215	0.253	0.467	36.0%	7,700	1.58	0.49	0.51
EGiB2	0.00527	0.214	0.253	0.467	42.2%	15,600	1.59	0.50	0.50

2.3 Chain-extension of poly(EGDEMA) or poly(EGDEMA-co-iBOMA) with Far

The dried poly(EGDEMA) or poly(EGDEMA-*co*-iBOMA) macroinitiators were dissolved in xylene in a 100 mL round-bottom flask and Far monomer was added. The formulations used for chain-extension with Far monomer to synthesize diblock copolymers are shown in Table 2. Similarly, reaction mixtures were purged with nitrogen for 30 mins, and reactions proceeded at 120°C for 120 to 300 mins depending on the desired final polymer chain length. Final block copolymers were precipitated using methanol, then dried in air overnight and in a vacuum oven at room temperature for a day.

Table 2: Recipes for poly(EGDEMA) and poly(EGDEMA-co-iBOMA) macroinitiator chain-extensions with Far at 120°C and polymer characterization.

Block copolymer ID	$m_{macroinitiator}$ (wt%)	m_{Far} (wt%)	m_{xylene} (wt%)	X_{Far}	Final M_n (g mol^{-1})	Final Đ
EG1-Far	7.14	42.9	50.0	35.0%	19,000	1.86
EG2-Far	22.0	28.0	50.0	23.0%	25,300	1.77
EGiB1-Far	8.00	42.0	50.0	32.0%	22,700	1.84
EGiB2-Far	11.9	38.1	50.0	33.0%	29,700	1.87

2.4 Thiol-ene clicking of block copolymers with thiol-POSS

Thiol-ene clicking of the poly(methacrylate-*b*-Far) block copolymers were done with mercaptopropyl isobutyl POSS (thiol-POSS) in 30 wt% polymer and POSS in toluene. About 2 g of polymer was dissolved in toluene, then either 10 or 20 molar equivalent of thiol-POSS to polymer chains was added with 0.5 wt% (relative to polymer and POSS) of AIBN initiator. Molar amounts of polymer were estimated using relative M_n values obtained from gel permeation chromatography (GPC) described in a later section. The mixture was purged with nitrogen for 30

mins and the reaction proceeded under nitrogen atmosphere with stirring at 80°C for 4 h. The final polymer was precipitated with methanol several times to remove unreacted POSS, then dried in air overnight and in a vacuum oven at room temperature for a day. The remaining double bonds of EGDEMA and Far after thiol-ene clicking were quantified using ^{1}H NMR. A summary of the characterized block copolymers after thiol-ene clicking is shown in Table 3.

*Table 3: Summary of poly(methacrylate-*b*-Far) block copolymers after thiol-ene clicking with thiol-POSS.*

Block copolymer ID	Molar equivalent of POSS [a]	Remaining EGDEMA C=C bonds	Remaining Far C=C bonds	Final M_n after clicking (g mol^{-1})	Final Đ after clicking
EG1-Far POSS10	10	54%	93%	25,900	1.52
EG1-Far POSS20	20	46%	94%	25,300	1.51
EG2-Far POSS10	10	46%	97%	38,500	1.39
EG2-Far POSS 20	20	74%	97%	41,700	1.83
EGiB1-Far POSS10	10	75%	90%	24,900	1.67
EGiB2-Far POSS 10	10	59%	95%	34,200	1.76

a) Amount of POSS added for thiol-ene clicking reactions were measured based on molar ratio of thiol:polymer chain and the moles of polymer were estimated using M_n from GPC analysis of the block copolymers.

2.5 Polymer characterization

Polymer samples (~0.15 mL) taken from the reaction mixtures for ^{1}H NMR and molecular weight analysis. Monomer conversion, copolymer composition, and amount of POSS clicked onto the polymer chains were determined from the NMR spectra, which are shown in Figure S.1-S.8 in Supporting Information. NMR samples were dissolved in $CDCl_3$ and were analyzed using the Bruker AVIIIHD 500 MHz spectrometer (16 scans). The final purified polymers after thiol-ene clicking showed that there was no residual unclicked POSS as indicated by the disappearance of the S-H proton at 1.3 ppm in the ^{1}H NMR spectra.

Number average molecular weight (M_n) and dispersity (Đ = M_w/M_n) of polymer samples were measured using gel permeation chromatography (GPC, Water Breeze) with HPLC grade THF as an eluent at a flow rate of 0.3 mL min^{-1}. The GPC has three Waters Styragel HR columns (HR1 with a molecular weight measurement range of 10^2 to 5×10^3 g mol^{-1}, HR2 with a molecular weight measurement range of 5×10^2 to 2×10^4 g mol^{-1}, and HR4 with a molecular weight measurement range of 5×10^3 to 6×10^5 g mol^{-1}), a guard column, and a refractive index (RI 2414) detector. The columns were heated to 40°C during analysis. The molecular weights were determined relative to poly(methyl methacrylate) (PMMA) calibration standards from Varian Inc. (ranging from 875 to 1,677,000 g mol^{-1}). The reported molecular weights were all relative to the PMMA standards and not adjusted with Mark–Houwink parameters.

2.6 Thermogravimetric analysis and differential scanning calorimetry

Thermogravimetric analysis (TGA) was done to determine thermal stability of the block copolymers with and without POSS using a Discovery 5500 TGA (TA Instruments). Polymer samples weighing between 5 – 10 mg were placed in platinum pans, and they were analyzed from room temperature to 500°C under nitrogen flow, then switched to air flow from 500 to 700°C at a rate of 10°C min^{-1}.

Glass transition temperatures (T_g) were determined using differential scanning calorimetry (DSC) Discovery 2500 from TA instruments. Polymer samples were heated up from room temperature to 200°C to remove any thermal history, then cooled to -90°C, then heated up to 200°C again to determine T_g. The heating rate used for all three cycles was 10°C min^{-1}.

2.7 Rheology

Rheological properties of the polymers were measured using the MCR302 rheometer (Anton Paar Instruments). The samples were placed between parallel plates with a gap of 1 mm, and storage (G′) and loss (G″) moduli were measured at an increasing shear strain from of 0.01 to 100% using 25 measurements at room temperature. Amplitude sweeps were also done to determine the shear strain range needed eventually for dynamic mechanical thermal analysis (DMTA). DMTA was done at a constant shear strain of 0.1% and frequency of 10 Hz from room temperature to 150°C at a rate of 10°C min^{-1} using the same parallel plate setup. Storage and loss moduli (G′ and G″) and damping factor ($\tan\delta$ = G″/G′) were measured accordingly using DMTA.

3 Results and discussion

*3.1 Poly(EGDEMA-*b*-Far) block copolymers clicked with thiol-POSS*

Initially, two poly(EGDEMA-*b*-Far) block copolymers (EG1-Far and EG2-Far) were synthesized, then clicked with thiol-POSS. The synthesis of the block copolymers began with the polymerization of EGDEMA to make macroinitiators. From literature, EGDEMA was not able to polymerize using SG1-based BlocBuilder or succinimidyl-modified BlocBuilder without the addition of 10 mol% of styrene [35]. The polymerization of EGDEMA using D7 initiator and no controlling comonomer showed linear kinetics (semi-logarithmic plots of conversion versus time) and molecular weight increased linearly with conversion as shown in Figure S.9. Molecular weights of up to 15,700 g mol^{-1} at low conversions (X~30-46%) were obtained with a Đ of ~1.5-1.6. Experimental M_n was consistently higher than the theoretical M_n, which indicates slow initiation but this was expected with D7 initiators, and is reflected in the higher Đ [39]. Nonetheless, the polymerization kinetic studies indicate adequate control of the homopolymerization of EGDEMA, and the resulting polymer was completely soluble in THF, showing there was no crosslinked material despite having a pendent norbornene double bond.

To further demonstrate effective control of the polymerization of EGDEMA using D7, the resulting macroinitiators were successfully chain-extended with Far to make diblock copolymers. The M_n increased from 7,700 and 15,700 g mol^{-1} for EG1 and EG2, respectively, to 19,000 and 25,300 g mol^{-1} after chain-extension as shown in Table 2. There was a clear shift in molecular weight distribution as shown in Figure 1, indicating most chains remained active and were able to

re-initiate and polymerize the Far block. The decrease in Đ is likely due to precipitation of the unreacted or dead macroinitiators that removed the shorter polymer chains, effectively narrowing the molecular weight distribution.

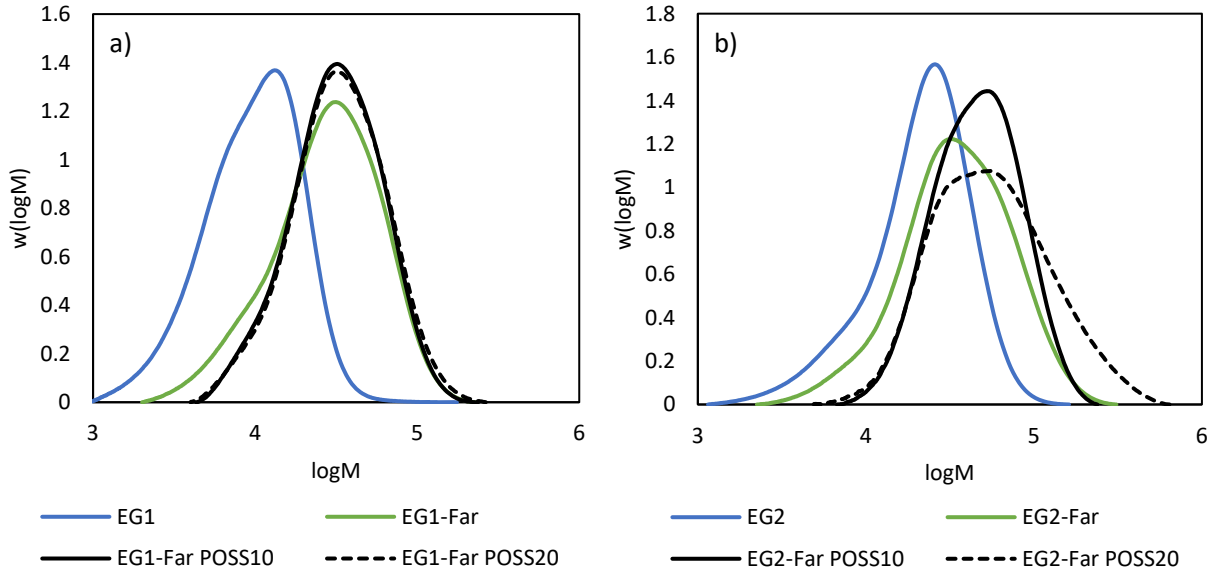

Figure 1: GPC traces of a) EG1-Far and b) EG2-Far block copolymers. The blue curves represent the poly(EGDEMA) macroinitiators, the green curves represent the chain-extended poly(EGDEMA-b-Far) block copolymers, and the black curves represent the block copolymers thiol-ene clicked with 10 and 20 molar equivalent of thiol-POSS.

Next, thiol-ene clicking was done on the block copolymers, where 10 and 20 molar equivalents of thiol-POSS to polymer chain was added to the reaction mixture dissolved in toluene. Thiol-ene clicking was done using thermally initiated radicals from AIBN decomposition at 80°C for 4 h. Afterwards, the final polymers were carefully purified to remove unreacted thiol-POSS by dissolving in small amount of THF and precipitated with minimal methanol until the solution was cloudy, indicating the start of phase separation. ^{1}H NMR showed the disappearance of S-H proton at 1.3 ppm and presence of the isobutyl groups from thiol-POSS in the final polymer, therefore showing the POSS groups were successfully attached to the polymer chains. Absence of unreacted POSS was also confirmed from GPC spectra. The molecular weights of EG1-Far and EG2-Far increased to ~25,000 and 40,000 g mol^{-1}, respectively, and the molecular weight distributions shifted once again as seen in Figure 1.

It is important to note that GPC traces reported in this study are relative molecular weights, therefore they actually represented the change in hydrodynamic volumes of the polymer chains after thiol-ene clicking. GPC traces obtained may not reflect the change in molecular weight, especially because the block copolymers were qualitatively measured according to the homopolymer calibrations [52]. The percentage of remaining double bonds as reported in Table 3 suggest higher degree of functionalization, when indeed, the ^{1}H NMR spectra (Figure S.7 and S.8) show much lower POSS functionalization and conjugation efficiency (defined here as percentage of thiol functionalization versus percentage of disappeared alkenes). The copolymer composition of POSS as determined from ^{1}H NMR of the final clicked copolymers are summarized in Table 4. The low conjugation efficiency was consistent with previous studies of functionalization of

poly(butadiene)-*co*-poly(ethylene oxide), which was attributed to cyclization of the thiol radical with the neighbouring pendent butadiene double bond via hydrogen abstraction [53, 54]. However, cyclization is very unlikely in this case because very large-membered rings would be formed between neighbouring EGDEMA units.

Table 4: Summary of block copolymer compositions after thiol-ene clicking from ^1H NMR.

Block copolymer ID	F_{Far}	F_{iBOMA}	F_{EGDEMA}	F_{POSS}
EG1-Far POSS10	0.775	-	0.192	0.033
EG1-Far POSS20	0.757	-	0.218	0.025
EG2-Far POSS10	0.770	-	0.122	0.103
EG2-Far POSS20	0.551	-	0.431	0.018
EGiB1-Far POSS10	0.689	0.296	0.270	0.041
EGiB2-Far POSS10	0.559	0.486	0.425	0.016

Many thiol-ene addition examples between small molecules, polymer-polymer conjugations, or functionalization of polymers with thiol molecules have shown that photo-initiated reactions exhibit higher conjugation efficiency and conversion with shorter reaction times compared to thermally initiated systems [55-58]. The general limitation to thiol-ene additions with thermally initiated radicals is the side reactions that occur, such as bimolecular radical termination. However, the low efficiency of thermally initiated systems was explained by the faster addition of initiator fragments onto the alkene relative to the abstraction of hydrogen from the thiol-radical [58]. Therefore, the conjugation efficiency is decreased due to the addition of initiator fragments as opposed to thiol functionalization. These side reactions can be alleviated by decreasing initiator concentration, which would slow down the rate of reaction, or increasing the thiol:ene ratio. Most thiol-ene functionalization of polymers utilize a 10:1 thiol:ene ratio, but this study used a 10:1 thiol:polymer chain ratio [53, 54, 59]. Notably, increasing the thiol-POSS:polymer ratio from 10 to 20 mol eq. did not increase functionalization significantly. Moreover, increasing the thiol-POSS:polymer ratio beyond 20 mol eq. was attempted, but due to the low thiol-ene clicking efficiency, it became difficult to separate unreacted POSS from the polymer. Therefore, photo-initiated thiol-ene clicking would have likely improved the efficiency of POSS functionalization in this study. Moreover, the bulky thiol-POSS groups likely provided extra steric hindrance, which further decreased conjugation efficiency.

Nonetheless, higher conversion of EGDEMA alkene bonds over Far alkene bonds suggest preferential clicking of thiol-POSS with EGDEMA over Far units. It was shown that terminal alkenes undergo thiol-ene clicking much more efficiently than internal *cis* alkenes and cyclic alkenes [60]. The functionalization of poly(1,2-butadiene) was much more efficient due to the 1,2-addition of butadiene, which ensures the double bond is at the end of the side groups [53, 54, 59]. Similarly, thiol-ene clicking of 1,2-addition isoprene units was much higher than 1,4-addition units [61, 62]. In this study, farnesene was polymerized mostly by 1,4-addition with the two other double bonds located internally on the pendent side chains, therefore the clicking of alkenes on poly(Far) was unlikely. Furthermore, thiol-ene reactions for norbornene have been shown to be very effective because the transition from a ring-strained alkene to a more flexible cyclic alkane is highly favoured [63, 64].

3.2 Poly(EGDEMA-co-iBOMA-b-Far) block copolymers clicked with thiol-POSS

Since most of the double bonds in the EGDEMA units were not able to click with thiol-POSS units, the unused EGDEMA units were then replaced with iBOMA units. There are several motivations for this: 1) poly(iBOMA) will add stiffness and mechanical strength to the block copolymers, and 2) iBOMA is also bio-sourced and may contribute from a sustainability viewpoint (however merely replacing a monomer feedstock with a renewable alternative should not be considered a sole sufficient criteria for making a process greener) [65]. Therefore, the poly(methacrylate) macroinitiators were synthesized by copolymerizing equimolar parts of EGDEMA and iBOMA monomers. The kinetics of the EGDEMA and iBOMA copolymerization were similar to the homopolymerization of EGDEMA, producing polymers of similar M_n and Đ at the same conditions as seen in Table 1. Additionally, the copolymer compositions of EGDEMA and iBOMA remained relatively constant and equal to the initial monomer composition throughout polymerization, which suggests the copolymerization is near the azeotropic composition, where there is negligible compositional drift. The copolymerization of EGDEMA and iBOMA also showed linear increase of M_n with conversion, suggesting good control of polymerization (Figure S.10).

The poly(EGDEMA-*co*-iBOMA) macroinitiators were successfully chain-extended with Far, indicating most polymer chains had active chain-ends. As seen in Figure 2, the molecular weight distributions of EGiB1 and EGiB2 clearly shifted after chain-extension with Far. However, after clicking EGiB1-Far and EGiB2-Far with 10 molar equivalents of thiol-POSS, not many POSS units were apparently added to the polymer chains as shown by the modest increase in molecular weight. This could have been due to the added steric hindrance from the iBOMA units, impeding POSS units from clicking with the double bonds of EGDEMA. Furthermore, adding iBOMA units also increase the stiffness of the polymer (discussed in a later section), which likely decreased polymer chain mobility and further impeded thiol-ene clicking of POSS. The final M_n after thiol-ene clicking with 10 mol eq. thiol-POSS for EGiB1-Far and EGiB2-Far were 24,900 and 34,200 g mol^{-1}, respectively. Similarly, the POSS functionalization of EGiB1-Far and EGiB2-Far block copolymers after thiol-ene clicking were fairly low compared to the remaining double bonds as seen from ^{1}H NMR shown in Table 4.

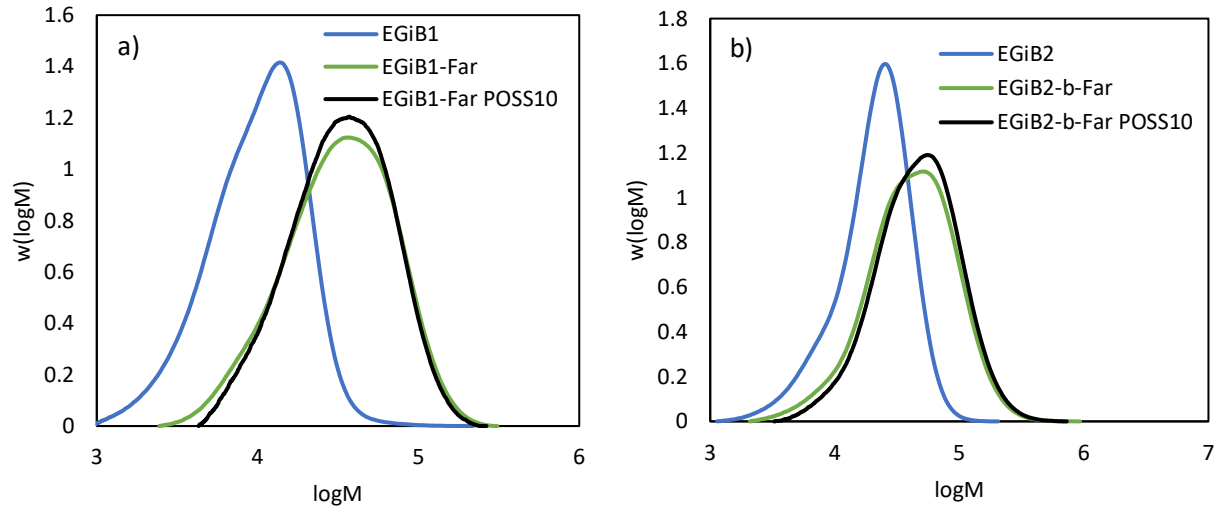

Figure 2: GPC traces of a) EGiB1-Far and b) EGiB2-Far block copolymers. The blue curves represent the poly(EGDEMA-co-iBOMA) macroinitiators, the green curves represent the chain-extended poly(EGDEMA-co-iBOMA-b-Far) block copolymers, and the black curves represent the block copolymers thiol-ene clicked with 10 molar equivalent of thiol-POSS.

3.3 Thermal stability of block copolymers with and without POSS

As thermoplastic elastomers are processible at high temperatures, it is important to understand their thermal stability and determine the processing temperature while avoiding decomposition of the material. TGA plots showing the decrease in weight with increasing temperature for poly(EGDEMA-*b*-Far) with and without POSS are shown in Figure 3. The decomposition temperature, or onset temperature (T_{onset}), is the temperature at which the mass of the polymer sample starts to decrease after a plateau. The endset temperature (T_{endset}) is the temperature at which the mass of polymer sample has reached close to zero. The T_{onset} and T_{endset} for all polymer samples are summarized in Table 5.

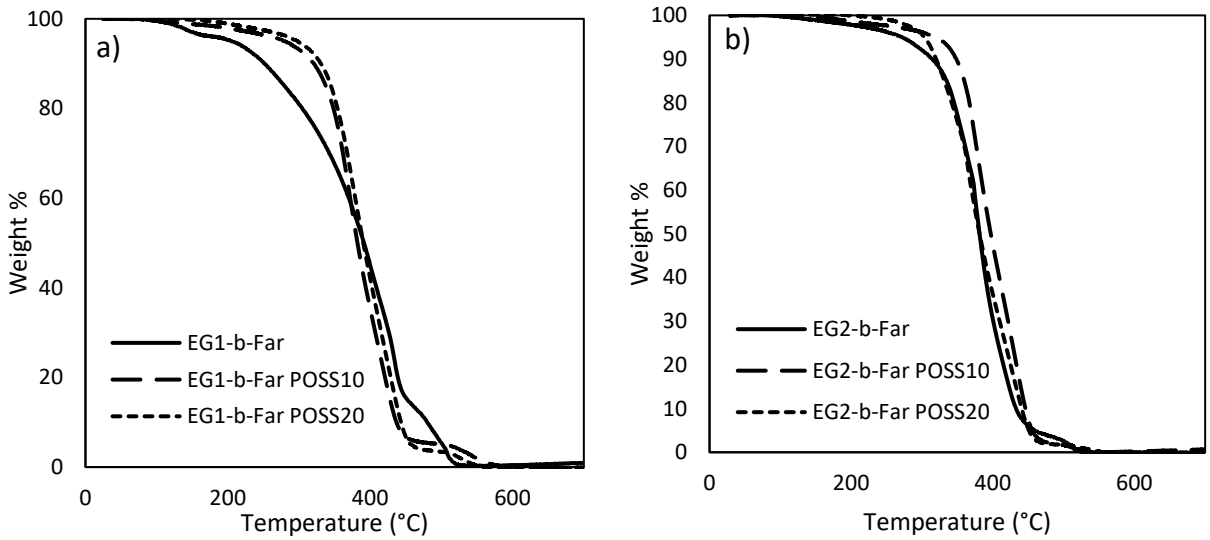

Figure 3: TGA plots of a) EG1-Far and b) EG2-Far block copolymers with and without POSS showing decrease in weight% with increasing temperature.

*Table 5: TGA results of poly(methacrylate-*b*-Far) block copolymers with and without added POSS.*

	EG1-Far			EG2-Far			EGiB1-Far		EGiB2-Far	
	No POSS [a]	10 mol eq. POSS	20 mol eq. POSS	No POSS	10 mol eq. POSS	20 mol eq. POSS	No POSS	10 mol eq. POSS	No POSS	10 mol eq. POSS
T_{onset} (°C)	120 298.2	335.2	335.5	351.2	351.1	334.0	315.0	310.2	301.0	315.6
T_{endset} (°C)	442.0	441.8	449.9	436.6	455.5	452.7	449.6	455.4	442.4	468.8

a) EG1-Far block copolymer with no POSS exhibited two-step degradation, therefore two T_{onset} values were reported.

Firstly, it is evident that the degradation curve for EG1-Far without POSS was a two-step degradation, whereas none of the other polymers exhibited the same behaviour. The first degradation step for EG1-Far began at around 120°C, then the second degradation occurred when the weight % decreased rapidly at around 298°C. Recall that EG1-Far has a very short poly(EGDEMA) block and mostly composed of poly(Far). This two-step degradation has been seen before with poly(myrcene), first at ~250°C which then decomposes quickly at ~425°C [29]. It was also observed with poly(styrene-*b*-myrcene-*b*-styrene) (SMS) triblock copolymer synthesized via RAFT, and the initial degradation was attributed to the depolymerization of poly(myrcene) with 1,4-addition, similar to poly(butadiene) with 1,4-conformation [66, 67]. However, in the cases for SMS block copolymers with longer poly(styrene) blocks, the initial degradation step was no longer evident. Furthermore, the thermal degradation of all block copolymers had 5-10 weight % of residual char until the nitrogen flow was switched to air flow at 500°C to completely decompose the residual mass. The residual char is typical of the decomposition of poly(butadiene) due to the depolymerization and thermally-induced crosslinking during degradation [68]. Both the poly(EGDEMA) and poly(Far) blocks in this study have remaining double bonds, therefore crosslinked residue is very likely. The residual char could be due to the decomposition of POSS as well [69].

It is apparent that by having a longer poly(EGDEMA) block (i.e. EG2-Far) or by linking the POSS moities to EG1-Far (i.e. EG1-Far POSS 10 and EG1-Far POSS20), the TGA curves only showed one degradation step. Interestingly, the degradation temperature of poly(EGDEMA) homopolymer synthesized by ATRP was reported to be 237°C, which is lower than what is observed for poly(EGDEMA-*b*-Far) in this study [44]. There seems to be a synergistic effect, where block copolymers help to minimize the initial degradation of poly(dienes) but also increase the thermal stability of poly(EGDEMA). This was also observed in a study examining the thermal degradation of poly(styrene-*b*-butadiene) diblock copolymers, where the block copolymers had a stabilization effect such that thermal stability is improved compared to a blend of the respective homopolymers [70]. This finding was explained by the delay of poly(styrene) degradation into toluene and styrene by-products due to the volatilization of poly(butadiene) into 1,3-butadiene and vinylcyclohexene, with the addition of methane and hydrogen. Perhaps, the degradation of EGDEMA was slowed down by decomposition of farnesene in this study.

For the block copolymers where the methacrylate blocks consisted of EGDEMA/iBOMA units, the addition of iBOMA also improved the thermal stability of the poly(Far) block such that the initial degradation is eliminated. EGiB1-Far and EG1-Far are similar in composition, where they have very short methacrylate blocks. As seen in Figure 4a) for EGiB1-Far without POSS compared to EG1-Far without POSS, the addition of iBOMA units increased the initial thermal degradation from 120 to 315°C. However, there is a weak indicator of a second degradation around 350°C for EGiB1-Far, which suggests some decomposition and release of the isobornyl group from the methacrylate backbone [45]. With POSS added to EGiB1-Far, the second decomposition of the isobornyl group was minimized. Similarly, in Figure 4b the degradation of EGiB2-Far shows as slight indication of the release of isobornyl groups at 350°C but was minimized with the addition of POSS.

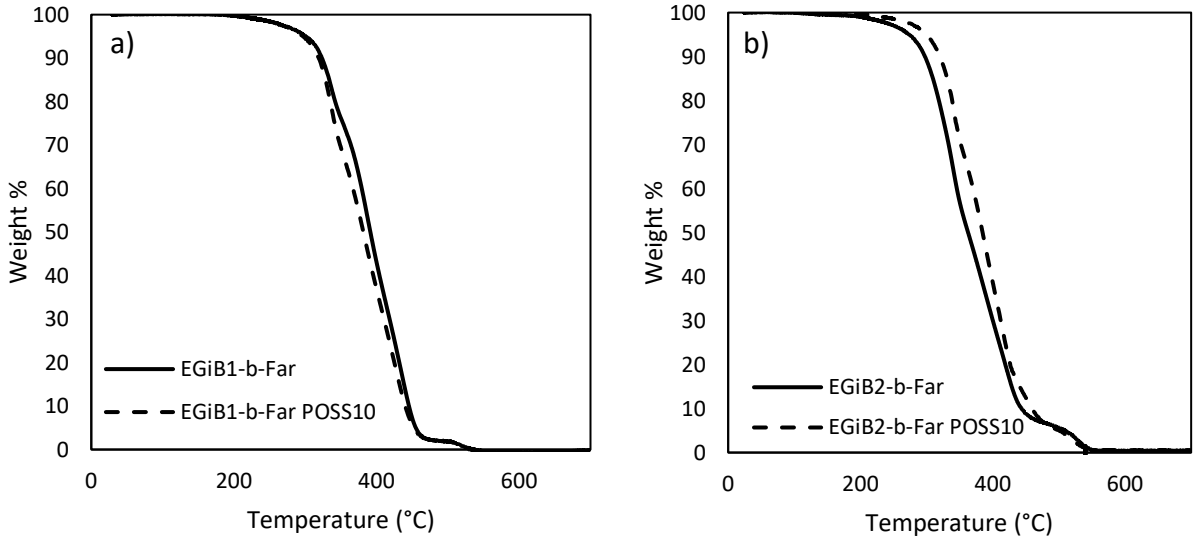

Figure 4: TGA plots of a) EGiB1-Far and b) EGiB2-Far block copolymers with and without POSS showing decrease in weight% with increasing temperature.

Otherwise, the decomposition temperature (T_{onset}) appeared to show negligible increase for block copolymers with added POSS compared to without (except for EG1-Far). This is likely due to the very low concentration of POSS that was added onto the polymer chains (1.6 to 10 mol%). In a study investigating the thermal stability of POSS-functionalized poly(ethylene), the increase in decomposition temperature depended on the substituents of the POSS units, as well as the type of bond that attaches the POSS to the polymer chain, but generally showed an improvement in thermal stability [50]. However, poly(ethylene) functionalized with POSS containing isobutyl R-groups and attached by a C_4H_8 alkyl chain did not show a significant increase in temperature at 5% weight loss ($T_{5\%}$). One study copolymerized styrene with POSS-functionalized styrene (F_{POSS} = 0.36-3.2 mol%) and reported an increase of 10°C in decomposition temperature at 10% weight loss ($T_{10\%}$) [71]. Conversely, in another study where poly(styrene) was functionalized with POSS groups (F_{POSS} = 1.1-1.4 mol%) post-polymerization showed negligible change in $T_{10\%}$ [72]. In an example most similar to our study, SEBS was functionalized with POSS via an azido group, and at most where there were 35 units of grafted POSS, the decomposition temperature increased ~20°C [51]. Therefore, it is difficult to conclude whether polymers functionalized with POSS would have a significant effect on overall thermal stability at such low concentrations.

Nonetheless, the addition of POSS improved the thermal degradation of Far diene units for EG1-Far block copolymers, as well as preventing the release of isobornyl groups for EGiB1-Far and EGiB2-Far block copolymers.

3.4 Rheology of block copolymers

Rheological tests were done to characterize viscoelastic properties of the block copolymers. Amplitude tests were performed at room temperature, where the polymer samples were placed between parallel plates, and the storage (G′) and loss (G″) moduli were measured with increasing shear strain. The G′ and G″ versus shear strain plots for the poly(EGDEMA-*b*-Far) block copolymers are compared in Figure 5.

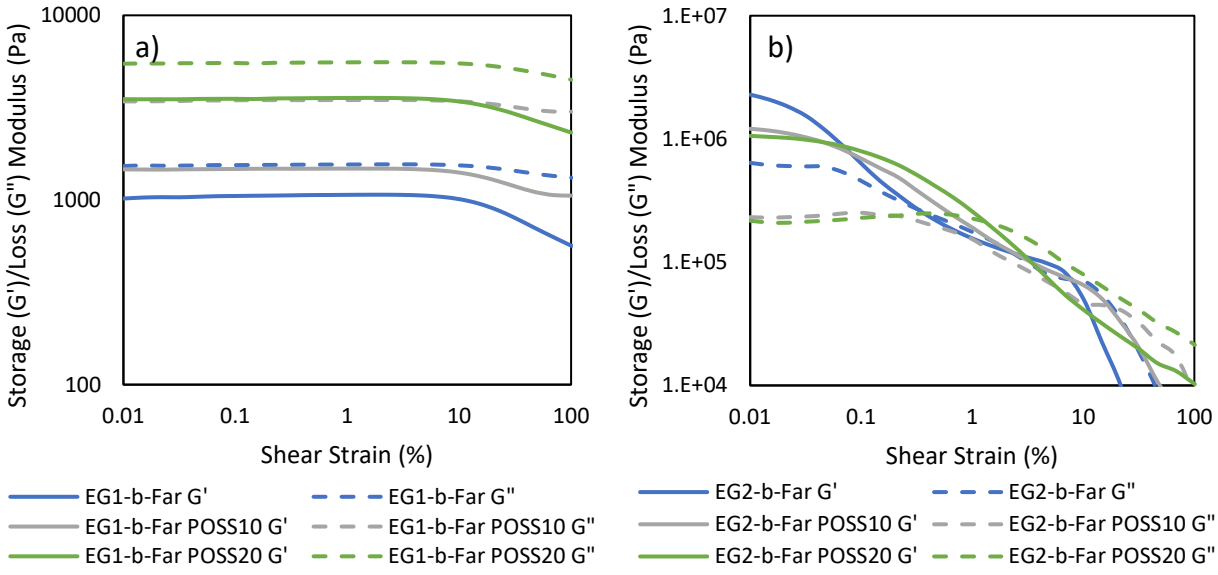

Figure 5: Storage (G') and loss (G") moduli versus shear strain plots for a) EG1-Far and b) EG2-Far block copolymers with and without POSS.

Since EG1-Far has a very short poly(EGDEMA) block, and the length of the poly(Far) block is well below its entanglement molecular weight of 50,000 g mol^{-1} [26], the block copolymer behaved like a very viscous liquid, even with added POSS. Furthermore, poly(EGDEMA) is a relatively soft polymer in comparison to other poly(methacrylates) as suggested by its T_g = 28°C [44]. As seen in Figure 5a, G″ is consistently higher than G′ for all EG1-Far samples indicating the polymers were indeed liquid-like. However, EG1-Far samples with added POSS show an increase in both storage and loss moduli, which indicates the mechanical strength of the block copolymers is increased even with low loadings of POSS. Furthermore, the linear viscoelastic (LVE) region was demonstrated by the plateau of G′ and G″ values up to a shear strain of 10%.

For the block copolymers with a longer poly(EGDEMA) block (M_n of poly(EGDEMA) macroinitiator was 15,700 g mol^{-1} versus 7,500 g mol^{-1}), EG2-Far, the polymer samples were solid at room temperature as they were able to be hot-pressed into disks of 1 mm thickness. In this case, G′ was greater than G″ at low shear strain as shown in Figure 5b, which indicate these polymers were more solid/gel-like. As shear strain increased, G′ crossed over with G″, suggesting flow and more liquid-like behaviour. A LVE region of G′ over a limited shear strain range was noticed for

EG2-Far. This region became more noticeable and sharper with increasing POSS as seen for EG2-Far POSS 10 and EG2-Far POSS20 and spanned over a wider shear strain range. The LVE regions exhibited by the EG2-Far polymers with and without POSS suggest the polymers behaved like a cross-linked material, but at higher shear strains, they flowed. This is indicative of a thermoplastic elastomer, which should behave like physically crosslinked polymer at ambient conditions but processible at high temperatures and/or shear. Furthermore, improved viscoelastic properties suggest that POSS was able to reinforce the physical crosslinks in these block copolymers, which is consistent with other thermoplastic elastomers either blended or functionalized with POSS [73, 74].

The EGiB1-Far and EGiB2-Far block copolymers, which include iBOMA units in the methacrylate block, display a LVE plateau region over an even wider range of shear strains compared to the EG2-Far block copolymers as seen in Figure 6. Similarly, G′ was greater than G″ indicating elastic solid-like materials, as EGiB1-Far and EGiB2-Far polymer samples were able to be hot pressed into solid discs as well. At higher shear strains > 1%, G′ crosses over with G″ and the polymers flowed. The broader plateaus were attributed to the more rigid isobornyl groups and higher T_g of poly(iBOMA) (190°C) that further reinforced the hard segments of the block copolymers [45]. However, there is negligible difference in the plateau regions for EGiB1-Far and EGiB2-Far with and without POSS since there was very little POSS added.

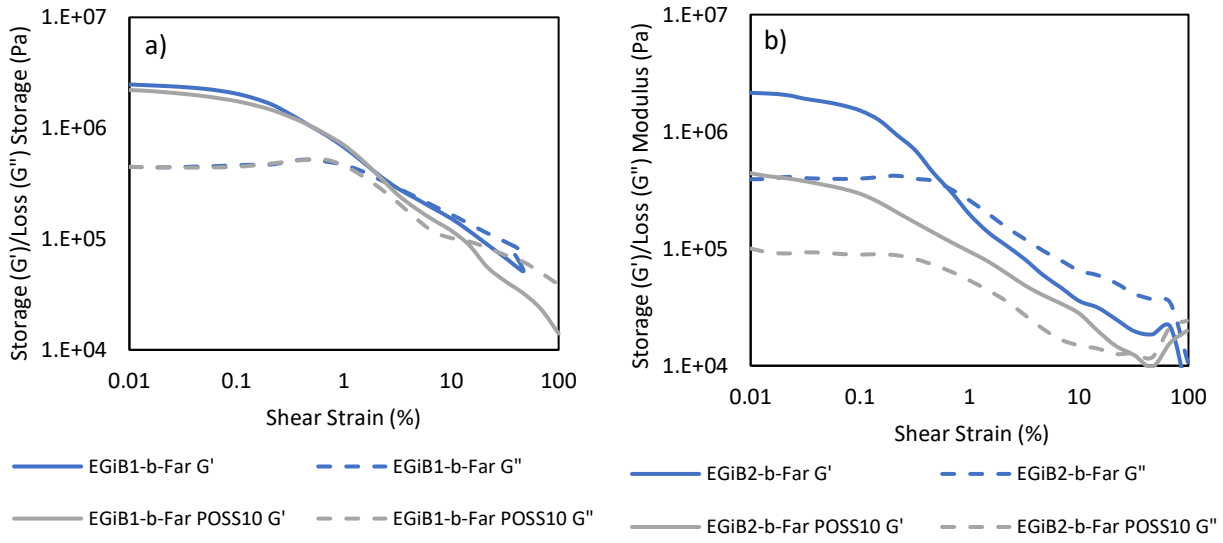

Figure 6: Storage (G') and loss (G") moduli versus shear strain plots for a) EGiB1-Far and b) EGiB2-Far block copolymers with and without POSS.

The addition of POSS made a significant improvement in viscoelastic properties for EG1-Far and EG2-Far block copolymers by providing mechanical strength in the poly(EGDEMA) segments and reinforcing the physical crosslinks. As for EGiB1-Far and EGiB2-Far, which have iBOMA copolymerized with EGDEMA statistically, the addition of POSS was very limited and therefore the mechanical properties remained relatively the same. Nonetheless, the addition of iBOMA did improve mechanical properties in comparison to EG1-Far and EG2-Far due to the rigid isobornyl groups of iBOMA. Furthermore, all block copolymers demonstrate glassy regions, which suggest the presence of physical crosslinks until higher shear strains were applied.

3.5 Glass transition temperatures of block copolymers

Glass transition temperatures of the block copolymers were determined thermally using DSC, as well as rheologically using DMTA. As the chiller for the rheometer could not reach below 0°C, sub-zero T_gs were not determined using DMTA. A summary of T_gs obtained are shown in Table 6. For all DSC endotherms, see Figure S.11-S.14 in Supporting Information.

Table 6: Glass transition temperatures of block copolymers measured using DSC and DMTA.

Differential Scanning Calorimetry (DSC)										
	EG1-Far			EG2-Far			EGiB1-Far		EGiB2-Far	
	No POSS	10 mol eq. POSS	20 mol eq. POSS	No POSS	10 mol eq. POSS	20 mol eq. POSS	No POSS	10 mol eq. POSS	No POSS	10 mol eq. POSS
T_g, (°C)	-71.6	-66.2	-64.2	-76.8 30.6	-70.5 31.3	-63.1 49.8	-72.0	-71.6	-67.8 91.3	-67.5 87.8
Dynamic Mechanical Temperature Analysis (DMTA)[a]										
T_g (°C)	-	-	-	63.3	72.2	71.2	109	115	123	123

a) T_gs reported using DMTA method in this table were obtained from the peak of tanδ versus temperature plots.

Examination of the DSC results indicated a distinct change in heat flow around -70°C for all block copolymers. This low T_g corresponds with the T_g of poly(Far) homopolymer in agreement with the literature value of -73°C [26]. The low T_g is also indicative of the soft, elastomeric segments of the block copolymers. However, a second T_g was not observed for the block copolymers with short poly(methacrylate) blocks (EG1-Far and EGiB1-Far), likely because the hard segments were not long enough to display a distinct second T_g and suggests some miscibility with the elastomeric phase. The block copolymers with longer poly(methacrylate) blocks exhibited two T_gs. The second T_g for EG2-Far with no POSS was observed at 30.6°C and corresponds to the T_g of poly(EGDEMA) homopolymer (T_g = 28°C) [44]. With the good agreement of the two T_gs (-76.8°C and 30.6°C) observed for EG2-Far with the T_gs of the homopolymers, it indicates possible microphase separation of the block copolymer.

The T_g from DMTA was obtained by determining the temperature at which tanδ = G″/G′ reaches its peak. Since EG1-Far block copolymers were already liquid-like at room temperature, the DMTA revealed only a continual decrease in G′ and G″ with temperature. According to the tanδ versus temperature plot in Figure 7a, there was a peak observed for all EG2-Far block copolymers above room temperature, which reconfirmed the second T_gs observed using DSC. Since sub-zero T_gs could not be measured with the rheometer, the first T_gs observed by DSC were not validated.

Nonetheless, T_gs acquired using DMTA were about 20°C higher than the second T_g values obtained from DSC for EG2-Far block copolymers. This discrepancy can be explained by the heterogeneity of the overall block copolymers that resulted in a distribution of relaxation times [75]. This was also observed with SBS polymers blended with POSS fillers, where there was a broadening of the

tanδ peak [73]. The increase in POSS fillers increased the breadth of the peak due to the segmental constraints and interactions between polymer chains and POSS additives. Furthermore, the block copolymers in this study have fairly high Đ especially compared to commercially available SBS, which usually have Đs closer to 1.1. Higher Đ indicates that not all polymer segments are the same length, which would also contribute to the distribution of relaxation times. Conversely, homopolymers show excellent agreement of T_gs between DSC and DMTA methods as seen for poly(Far) [26].

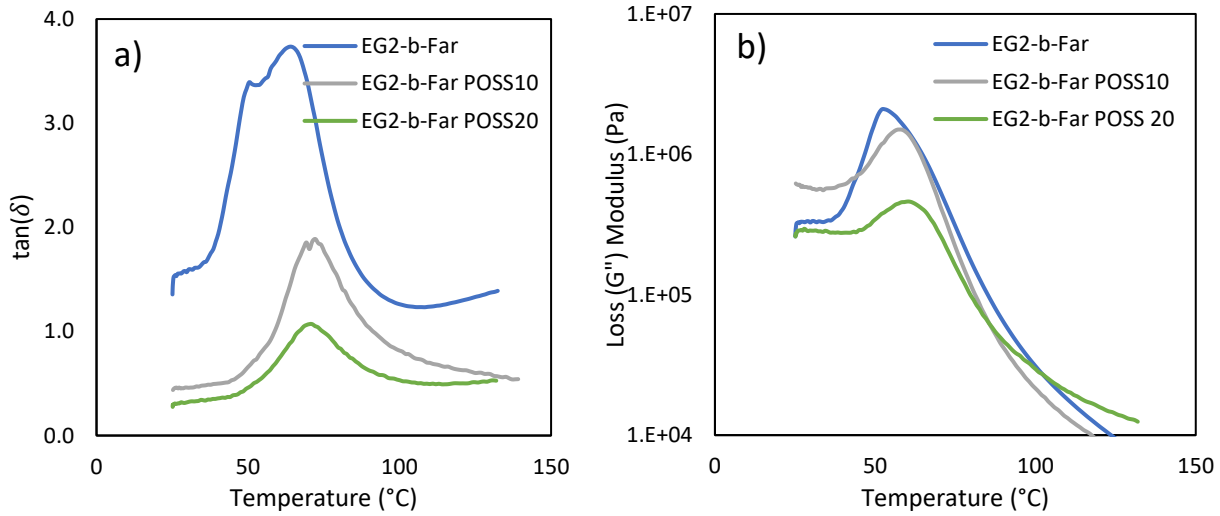

Figure 7: DMTA of EG2-Far block copolymers with and without POSS, where a) tanδ and b) loss modulus are plotted as a function of temperature.

Some have argued that the temperature at which G″ is at its maximum is the more accurate T_g measurement, particularly for polymer mixtures because G″ is the measure of dissipation, which is the transition temperature being considered [76]. In Figure 7b, the T_gs where G″ is at its peak are 51°C, 57°C, and 60°C, which are much closer to the second T_gs obtained by DSC for EG2-Far block copolymers. Nevertheless, the trend is the same using all methods of T_g determination, and that is an increase in T_g with increasing POSS added for all block copolymers. This is consistent with other examples of polymers with added POSS, as POSS decreased chain mobility and increased the rigidity of the polymer chains [49, 73, 77]. However, in the case of polyurethane thermoplastic elastomers, the functionalization with POSS disrupted the crystallinity of the hard segments such that the T_gs were decreased [74].

The second T_gs obtained for EGiB1-Far block copolymers were not as straightforward. As shown in Table 5, a second T_g was not observed using DSC. However, from DMTA, there appears to be local maximum tanδ values observed around 110°C in Figure 8a, after which tanδ increased very quickly. This may suggest a second T_g for the EGiB1-Far block copolymers, but it is not definitive. Furthermore, the liquid-like behaviour of the block copolymers is very much influenced by the soft poly(Far) block, especially because EGiB1-Far is largely made of poly(Far) that is below its entanglement molecular weight. It is plausible that the second T_g could be as high as 110°C, since poly(EGDEMA) and poly(iBOMA) have T_gs of 28°C and 190°C, respectively, so the T_g of the statistical EGDEMA/iBOMA copolymer segment is expected to be in between the two values [44, 45]. However, the T_g of poly(iBOMA) could range from 170°C to 206°C depending on tacticity

[78]. Examining G″ in Figure 8b, modest maxima were observed as well and T_gs were estimated as 67°C and 69°C for EGiB1-Far and EGiB1-Far POSS 10, respectively.

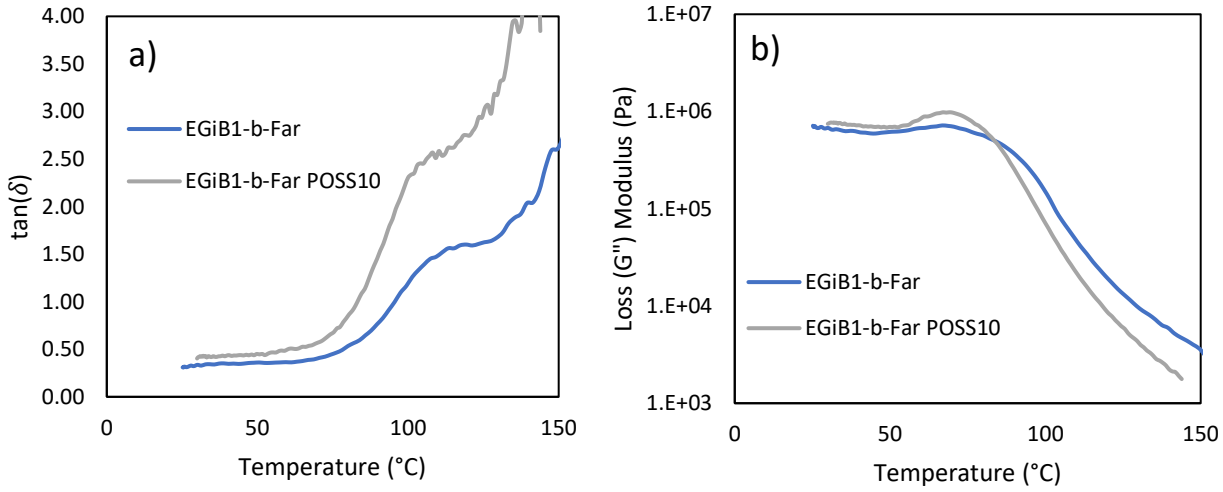

Figure 8: DMTA of EGiB1-Far block copolymers with and without POSS, where a) tanδ and b) loss modulus are plotted as a function of temperature.

Similar to EG2-Far block copolymers, more than one T_g for EGiB2-Far was observed due to the longer poly(methacrylate) blocks. From DSC, there were two T_gs observed for both EGiB2-Far (-67.8°C and 91.3°C) and EGiB2-Far POSS10 (-67.5°C and 87.8°C). The first T_gs observed at around -67°C corresponds with the T_g of poly(Far) homopolymer and the second T_gs fall in between the T_gs of poly(EGDEMA) and poly(iBOMA) homopolymers. According to the Gordon-Taylor equation, random copolymers would exhibit a T_g between the T_g of the two homopolymers [79]. Furthermore, compositional drift was not observed with the copolymerization of EGDEMA and iBOMA, since there was an equimolar concentration of each monomer initially and the copolymer composition was also nearly equimolar, which further confirms its random composition, rather than a gradient microstructure. It is important to note that for EGiB2-Far block copolymers, the addition of POSS had negligible effect on T_gs, likely because out of all the polymer samples, EGiB2-Far block copolymers had the least amount of POSS incorporated at 1.6 mol%.

The DMTA for EGiB2-Far block copolymers revealed much more pronounced tanδ peaks (Figure 9a) compared to EGiB1-Far block copolymers. Due to the longer poly(EGDEMA-*co*-iBOMA) blocks, the overall behaviour was less influenced by the flow behaviour of poly(Far) blocks, and therefore obvious tanδ peaks were observed. In Figure 9a, the temperature at which tanδ had reached its peak is at 123°C for both EGiB2-Far with and without POSS. Once again, comparing to T_gs obtained by DSC, T_gs observed in the tanδ plots are higher. However, for both DSC and DMTA, the T_gs that correspond to the poly(methacrylate) blocks did not differ very much with or without POSS. The peaks in G″ as shown in Figure 9b indicate T_gs of 108°C and 103°C for EGiB2-Far and EGiB2-Far POSS10, respectively, which also do not show a great difference between samples with and without POSS. Furthermore, the T_gs observed for the poly(EGDEMA-*co*-iBOMA) blocks using DMTA, regardless of block length (EGiB1-Far versus EGiB2-Far), are very similar.

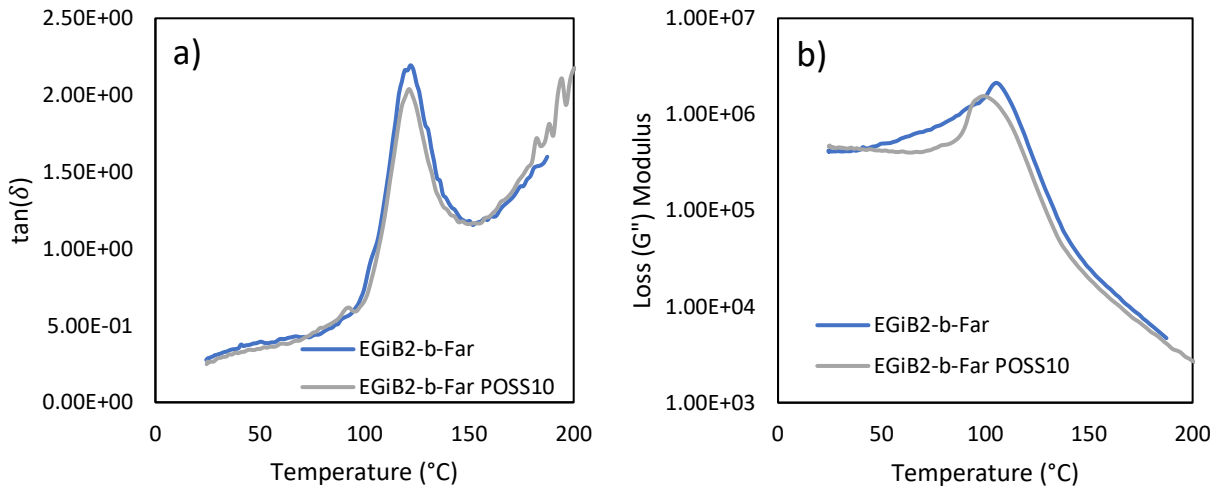

Figure 9: DMTA of EGiB2-Far block copolymers with and without POSS, where a) tanδ and b) loss modulus are plotted as a function of temperature.

Two T_gs were not observed for EG1-Far due to the short poly(EGDEMA) block, therefore a second T_g was not observed in both DSC and DMTA. Otherwise, the use of DSC and DMTA confirmed distinct T_gs of the diblock copolymers corresponding to their respective blocks. The addition of POSS resulted in an increase in T_g for EG1-Far and EG2-Far block copolymers for both the poly(Far) and poly(EGDEMA) blocks. For the block copolymers with added iBOMA in the poly(methacrylate) blocks, the addition of POSS showed negligible difference in T_g, since the concentration of POSS was fairly low. Additionally, the transition behaviour could have been dominated by the rigid iBOMA units such that the little POSS added made negligible difference. Nevertheless, distinct T_gs could suggest possible microphase separation for most of these block copolymers, namely EG2-Far, EGiB1-Far, and EGiB2-Far with and without POSS.

To further investigate whether there is microphase separation, polymer films were prepared in the hot press at 120°C for EG2-Far block copolymers and at 160°C for EGiB2-Far block copolymers and cooled slowly overnight to room temperature for small angle X-ray scattering (SAXS) analysis. Higher order peaks were not observed that would be indicative of self-assembled structures. The Flory-Huggins enthalpic interaction parameter, χ, was estimated using (1) to provide some insight regarding the miscibility between the two block segments.

$$\chi_{AB} = \frac{\bar{V}}{RT}(\delta_A - \delta_B)^2 \quad (1)$$

The interactions of polymers A and B depend on molar volume of the polymer, $\bar{V}$, the solubility parameters, δ_A and δ_B, of the respective monomers, and temperature, T. The molar volume of a mixture is determined by $\bar{V} = \sqrt{\overline{V_A V_B}}$. For block copolymers, $\chi N \approx 10.5$ denotes the order-disorder transition, where N is overall degree of polymerization [80]. Solubility parameters and molar volumes of some relevant related monomers are summarized in Table 7. The solubility parameter of Far and EGDEMA were not found in literature and were calculated based on group component contributions method based on the Hoftyzer-Van Krevelen methodology [81]. Far has a similar solubility parameter compared to other dienes such as butadiene, isoprene, and myrcene. An approximate χ was calculated between Far and EGDEMA to be 0.0068 at 120°C (the temperature

at which poly(EGDEMA-*b*-Far) polymers were processed before conducting SAXS). Far and EGDEMA in EG1-Far and EG2-Far block copolymers have similar solubility parameters, and therefore have a low χ and suggest miscibility. Far and iBOMA have a much higher χ of 0.35 at 160°C (the temperature at which poly(EGDEMA-*co*-iBOMA-*b*-Far) polymers were processed before conducting SAXS)., however this only suggests that iBOMA and Far have greater immiscibility, but cannot be correlated to the case of EGiB1-Far and EGiB2-Far since the methacrylate blocks are random copolymers of EGDEMA and iBOMA.

Table 7: Summary of solubility parameters and molar volumes of relevant monomers.

Monomer	δ (MPa$^{1/2}$)	$\bar{V}$ (cm^3 mol^{-1})
Butadiene (BD)	16.6 [a]	60.7 [a]
Isoprene (IP)	16.2 [a]	75.7 [a]
Myrcene (Myr)	16.4 [b]	170 [e]
Farnesene (Far)	14.4 [c]	251 [e]
Styrene (St)	17.4 [a]	98 [a]
iBOMA	16.7 [d]	226 [e]
EGDEMA	14.1 [c]	246 [e]

a) Values obtained from literature.[81]
b) Solubility parameter was estimated in literature.[82]
c) Solubility parameters of farnesene and EGDEMA were calculated based on Hoftyzer-Van Krevelen's Component Group Contributions method.
d) Solubility parameter of iBOMA obtained from literature.[83]
e) Molar volumes were calculated based on density and molar mass of monomers.

For reference, typical SBS is made of poly(styrene) blocks with M_n ~ 10-20,000 g mol^{-1} and poly(butadiene) blocks with M_n ~40-80,000 g mol^{-1} [84]. The χ between poly(styrene) and poly(butadiene) was calculated at 120°C (20°C above T_g of polystyrene) to be 0.015 [30]. In addition to the higher interaction parameter, the high degrees of polymerization for SBS further enables phase separation. The N of the block copolymers in this study are fairly short in comparison to SBS and would require much higher degrees of polymerization to enthalpically induce ordered phase separation [80]. However, distinct T_gs measured in DSC and DMTA still suggest some microphase separation, but the block copolymers are likely weakly segregated and disordered as suggested by SAXS and χ approximations.

4 Conclusions

The polymerization of EGDEMA by nitroxide-mediated polymerization using D7 initiator was done for the first time, where no controlling comonomer was required and chain-ends remained active for chain-extension regardless of high Đ (~1.5-1.6). The poly(EGDEMA) macroinitiators

were re-initiated for polymerization of Far, a bio-based terpene that is similar in structure to petroleum-derived butadiene and isoprene. Similarly, the poly(methacrylate) blocks were also synthesized by statistically copolymerizing EGDEMA and iBOMA to form a more rigid methacrylate block. Since EGDEMA has a pendent double bond on the norbornene group, this allowed for thiol-ene clicking with thiol-POSS units onto the block copolymers post-polymerization. Although the conjugation efficiency of the thermal initiated thiol-ene clicking was low, ^{1}H NMR showed that thiol-POSS preferentially clicked onto the double bond of EGDEMA and not Far.

Despite the low fraction of POSS incorporation (1.6 – 10 mol% incorporation of POSS), the thermal stability of the poly(Far) blocks was improved and the degradation of isobornyl groups for polymers containing iBOMA units was reduced. These block copolymers containing POSS demonstrated increased mechanical strength as shown by the increase in modulus due to the reinforced physical crosslinks provided by POSS in the poly(methacrylate) blocks. Furthermore, distinct T_gs were observed using DSC and DMTA for the block copolymers containing longer poly(methacrylate) blocks (around -70°C for the rubbery poly(Far) blocks and up to 110°C for the thermoplastic poly(methacrylate) blocks). This suggests microphase separation, even though microphase morphology was not observed, likely due to the relatively small degrees of polymerization. Nonetheless, incorporation of POSS increased the T_g of the respective blocks, which confirms the presence of reinforced physical crosslinks and increased stiffness due to the POSS units. Therefore, these novel block copolymers that were easily functionalized with POSS by thiol-ene clicking show good potential eventually for applications as TPEs.

5 Acknowledgements

The authors thank the Natural Sciences and Engineering Research Council of Canada (NSERC) for funding this research (NSERC Discovery Grant 288125). The authors also acknowledge Dr. Robin Stein and Dr. Hatem Titi at the McGill Chemistry Material Characterization facility for running NMR and SAXS samples for analysis. The facility and staff are supported by the Quebec Centre of Advanced Materials. Their help was greatly appreciated during a time with COVID restrictions and limited access. The authors also deeply thank Derek McPhee of Amyris for facilitating the delivery of the farnesene used in this study.

6 References

[1] J.G. Drobny, 1. Introduction, Handbook of Thermoplastic Elastomers (2nd Edition), Elsevier2014.
[2] E.N. Kresge, Polyolefin Thermoplastic Elastomer Blends, Rubber Chemistry and Technology 64(3) (1991) 469-480.
[3] A.K. Gupta, S.N. Purwar, Crystallization of PP in PP/SEBS blends and its correlation with tensile properties, Journal of Applied Polymer Science 29(5) (1984) 1595-1609.
[4] B. Ohlsson, B. Törnell, Melt miscibility in blends of polypropylene, polystyrene-block-poly(ethylene-stat-butylene)-block-polystyrene, and processing oil from melting point depression, Polymer Engineering & Science 36(11) (1996) 1547-1556.

[5] C.A. Sierra, C. Galán, J.G. Fatou, M.D. Parellada, J.A. Barrio, Thermal and mechanical properties of poly (styrene-b-ethylene-co-butylene-b-styrene) triblock copolymers, Polymer 38(17) (1997) 4325-4335.
[6] A.F. Johnson, D.J. Worsfold, Anionic polymerization of butadiene and styrene, Journal of Polymer Science Part A: General Papers 3(2) (1965) 449-455.
[7] R. Bening, D. Handlin, L. Sterna, C. Willis, Novel block copolymers and method for making same, Kraton Polymers US LLC, 2003.
[8] M. Morton, L.J. Fetters, Homogeneous anionic polymerization of unsaturated monomers, Journal of Polymer Science: Macromolecular Reviews 2(1) (1967) 71-113.
[9] M. Morton, L.J. Fetters, E.E. Bostick, Mechanisms of homogeneous anionic polymerization by alkyllithium initiators, Journal of Polymer Science Part C: Polymer Symposia 1(1) (1963) 311-323.
[10] D. Jenkins Aubrey, G. Jones Richard, G. Moad, Terminology for reversible-deactivation radical polymerization previously called "controlled" radical or "living" radical polymerization (IUPAC Recommendations 2010), Pure and Applied Chemistry, 2009, p. 483.
[11] D.A. Shipp, Reversible-Deactivation Radical Polymerizations, Polymer Reviews 51(2) (2011) 99-103.
[12] K. Matyjaszewski, Atom Transfer Radical Polymerization (ATRP): Current Status and Future Perspectives, Macromolecules 45(10) (2012) 4015-4039.
[13] H.-S. Yu, J.-S. Kim, V. Vasu, C.P. Simpson, A.D. Asandei, Cu-Mediated Butadiene ATRP, ACS Catalysis 10(12) (2020) 6645-6663.
[14] Y.-F. Zhu, F.-J. Jiang, P.-P. Zhang, J. Luo, H.-D. Tang, Atom transfer radical polymerization and copolymerization of isoprene catalyzed by copper bromide/2,2′-bipyridine, Chinese Chemical Letters 27(6) (2016) 910-914.
[15] J. Chiefari, Y.K. Chong, F. Ercole, J. Krstina, J. Jeffery, T.P.T. Le, R.T.A. Mayadunne, G.F. Meijs, C.L. Moad, G. Moad, E. Rizzardo, S.H. Thang, Living Free-Radical Polymerization by Reversible Addition−Fragmentation Chain Transfer: The RAFT Process, Macromolecules 31(16) (1998) 5559-5562.
[16] S. Harrisson, X. Liu, J.-N. Ollagnier, O. Coutelier, J.-D. Marty, M. Destarac, RAFT Polymerization of Vinyl Esters: Synthesis and Applications, Polymers 6(5) (2014) 1437.
[17] M.K. Georges, R.P.N. Veregin, P.M. Kazmaier, G.K. Hamer, Narrow molecular weight resins by a free-radical polymerization process, Macromolecules 26(11) (1993) 2987-2988.
[18] M.K. Georges, G.K. Hamer, N.A. Listigovers, Block Copolymer Synthesis by a Nitroxide-Mediated Living Free Radical Polymerization Process, Macromolecules 31(25) (1998) 9087-9089.
[19] M.B. Kolicheski, L.C. Cocco, D.A. Mitchell, M. Kaminski, Synthesis of myrcene by pyrolysis of β-pinene: Analysis of decomposition reactions, Journal of Analytical and Applied Pyrolysis 80(1) (2007) 92-100.
[20] H. Zheng, J. Chen, C. Li, J. Chen, Y. Wang, S. Zhao, Y. Zeng, Mechanism and kinetics of the pyrolysis of β-pinene to myrcene, Journal of Analytical and Applied Pyrolysis 123 (2017) 99-106.
[21] M. Eisenacher, S. Beschnitt, W. Hölderich, Novel route to a fruitful mixture of terpene fragrances in particular phellandrene starting from natural feedstock geraniol using weak acidic boron based catalyst, Catalysis Communications 26 (2012) 214-217.
[22] G. Brieger, Convenient preparation of trans-β-farnesene, The Journal of Organic Chemistry 32(11) (1967) 3720-3720.

[23] G. Brieger, T.J. Nestrick, C. McKenna, Synthesis of trans, trans-.alpha.-farnesene, The Journal of Organic Chemistry 34(12) (1969) 3789-3791.
[24] M.I. Hulnik, I.V. Vasilenko, A.V. Radchenko, F. Peruch, F. Ganachaud, S.V. Kostjuk, Aqueous cationic homo- and co-polymerizations of β-myrcene and styrene: a green route toward terpene-based rubbery polymers, Polymer Chemistry 9(48) (2018) 5690-5700.
[25] C. Zhou, Z. Wei, C. Jin, Y. Wang, Y. Yu, X. Leng, Y. Li, Fully biobased thermoplastic elastomers: Synthesis of highly branched linear comb poly(β-myrcene)-graft-poly(l-lactide) copolymers with tunable mechanical properties, Polymer 138 (2018) 57-64.
[26] C. Iacob, T. Yoo, J. Runt, Molecular Dynamics of Polyfarnesene, Macromolecules 51(13) (2018) 4917-4922.
[27] T. Yoo, S.K. Henning, Synthesis and characterization of farnesene-based polymers, Rubber Chemistry and Technology 90(2) (2017) 308-324.
[28] S.B. Luk, L.A. Azevedo, M. Maric, Reversible deactivation radical polymerization of bio-based dienes, Reactive and Functional Polymers 162 (2021) 104871.
[29] P. Sarkar, A.K. Bhowmick, Synthesis, characterization and properties of a bio-based elastomer: polymyrcene, RSC Advances 4(106) (2014) 61343-61354.
[30] J. Brandrup, E.H. Immergut, E.A. Grulke, Polymer handbook, 4th ed. ed., Wiley, New York, 1999.
[31] L.J. Fetters, D.J. Lohse, D. Richter, T.A. Witten, A. Zirkel, Connection between Polymer Molecular Weight, Density, Chain Dimensions, and Melt Viscoelastic Properties, Macromolecules 27(17) (1994) 4639-4647.
[32] S.B. Luk, M. Marić, Nitroxide-Mediated Polymerization of Bio-Based Farnesene with a Functionalized Methacrylate, Macromolecular Reaction Engineering 13(3) (2019) 1800080.
[33] S.B. Luk, M. Maríc, Polymerization of Biobased Farnesene in Miniemulsions by Nitroxide-Mediated Polymerization, ACS Omega 6(7) (2021) 4939-4949.
[34] A. Métafiot, J.-F. Gérard, B. Defoort, M. Marić, Synthesis of β-myrcene/glycidyl methacrylate statistical and amphiphilic diblock copolymers by SG1 nitroxide-mediated controlled radical polymerization, Journal of Polymer Science Part A: Polymer Chemistry 56(8) (2018) 860-878.
[35] A. Maupu, Y. Kanawati, A. Métafiot, M. Maric, Ethylene Glycol Dicyclopentenyl (Meth)Acrylate Homo and Block Copolymers via Nitroxide Mediated Polymerization, Materials 12(9) (2019).
[36] Y. Guillaneuf, D. Gigmes, S.R.A. Marque, P. Tordo, D. Bertin, Nitroxide-Mediated Polymerization of Methyl Methacrylate Using an SG1-Based Alkoxyamine: How the Penultimate Effect Could Lead to Uncontrolled and Unliving Polymerization, Macromolecular Chemistry and Physics 207(14) (2006) 1278-1288.
[37] B. Charleux, J. Nicolas, O. Guerret, Theoretical Expression of the Average Activation−Deactivation Equilibrium Constant in Controlled/Living Free-Radical Copolymerization Operating via Reversible Termination. Application to a Strongly Improved Control in Nitroxide-Mediated Polymerization of Methyl Methacrylate, Macromolecules 38(13) (2005) 5485-5492.
[38] J. Nicolas, C. Dire, L. Mueller, J. Belleney, B. Charleux, S.R.A. Marque, D. Bertin, S. Magnet, L. Couvreur, Living Character of Polymer Chains Prepared via Nitroxide-Mediated Controlled Free-Radical Polymerization of Methyl Methacrylate in the Presence of a Small Amount of Styrene at Low Temperature, Macromolecules 39(24) (2006) 8274-8282.

[39] N. Ballard, M. Aguirre, A. Simula, A. Agirre, J.R. Leiza, J.M. Asua, S. van Es, New Class of Alkoxyamines for Efficient Controlled Homopolymerization of Methacrylates, ACS Macro Letters 5(9) (2016) 1019-1022.
[40] N. Ballard, A. Simula, M. Aguirre, J.R. Leiza, S. van Es, J.M. Asua, Synthesis of poly(methyl methacrylate) and block copolymers by semi-batch nitroxide mediated polymerization, Polymer Chemistry 7(45) (2016) 6964-6972.
[41] A.L. Hook, C.-Y. Chang, J. Yang, J. Luckett, A. Cockayne, S. Atkinson, Y. Mei, R. Bayston, D.J. Irvine, R. Langer, D.G. Anderson, P. Williams, M.C. Davies, M.R. Alexander, Combinatorial discovery of polymers resistant to bacterial attachment, Nature Biotechnology 30(9) (2012) 868-875.
[42] B.J. Tyler, A. Hook, A. Pelster, P. Williams, M. Alexander, H.F. Arlinghaus, Development and characterization of a stable adhesive bond between a poly(dimethylsiloxane) catheter material and a bacterial biofilm resistant acrylate polymer coating, Biointerphases 12(2) (2017) 02C412.
[43] F. Koschitzki, R. Wanka, L. Sobota, J. Koc, H. Gardner, K.Z. Hunsucker, G.W. Swain, A. Rosenhahn, Amphiphilic Dicyclopentenyl/Carboxybetaine-Containing Copolymers for Marine Fouling-Release Applications, ACS Applied Materials & Interfaces 12(30) (2020) 34148-34160.
[44] P. Mandal, N.K. Singha, Tailor-made polymethacrylate bearing bicyclo-alkenyl functionality via selective ATRP at ambient temperature and its post-polymerization modification by 'thiol–ene' reaction, RSC Advances 4(11) (2014) 5293-5299.
[45] A. Matsumoto, K. Mizuta, T. Otsu, Synthesis and thermal properties of poly(cycloalkyl methacrylate)s bearing bridged- and fused-ring structures, Journal of Polymer Science Part A: Polymer Chemistry 31(10) (1993) 2531-2539.
[46] P. Mandal, S. Choudhury, N.K. Singha, Acrylic ABA triblock copolymer bearing pendant reactive bicycloalkenyl functionality via ATRP and tuning its properties using thiol-ene chemistry, Polymer 55(22) (2014) 5576-5583.
[47] E. Ayandele, B. Sarkar, P. Alexandridis, Polyhedral Oligomeric Silsesquioxane (POSS)-Containing Polymer Nanocomposites, Nanomaterials 2(4) (2012).
[48] W. Zhang, G. Camino, R. Yang, Polymer/polyhedral oligomeric silsesquioxane (POSS) nanocomposites: An overview of fire retardance, Progress in Polymer Science 67 (2017) 77-125.
[49] P.T. Mather, H.G. Jeon, A. Romo-Uribe, T.S. Haddad, J.D. Lichtenhan, Mechanical Relaxation and Microstructure of Poly(norbornyl-POSS) Copolymers, Macromolecules 32(4) (1999) 1194-1203.
[50] P. Groch, K. Dziubek, K. Czaja, M. Grzymek, Investigation of thermal stability of ethylene copolymers with POSS - Study under static and dynamic conditions, Polymer Degradation and Stability 156 (2018) 218-227.
[51] M. Niu, R. Xu, P. Dai, Y. Wu, Novel hybrid copolymer by incorporating POSS into hard segments of thermoplastic elastomer SEBS via click coupling reaction, Polymer 54(11) (2013) 2658-2667.
[52] K. Philipps, T. Junkers, J.J. Michels, The block copolymer shuffle in size exclusion chromatography: the intrinsic problem with using elugrams to determine chain extension success, Polymer Chemistry (2021).
[53] J. Justynska, Z. Hordyjewicz, H. Schlaad, Toward a toolbox of functional block copolymers via free-radical addition of mercaptans, Polymer 46(26) (2005) 12057-12064.
[54] J. Justynska, Z. Hordyjewicz, H. Schlaad, New Functional Diblock Copolymers Through Radical Addition of Mercaptans, Macromolecular Symposia 240(1) (2006) 41-46.

[55] M. Uygun, M.A. Tasdelen, Y. Yagci, Influence of Type of Initiation on Thiol–Ene "Click" Chemistry, Macromolecular Chemistry and Physics 211(1) (2010) 103-110.
[56] B.D. Fairbanks, D.M. Love, C.N. Bowman, Efficient Polymer-Polymer Conjugation via Thiol-ene Click Reaction, Macromolecular Chemistry and Physics 218(18) (2017) 1700073.
[57] L.M. Campos, K.L. Killops, R. Sakai, J.M.J. Paulusse, D. Damiron, E. Drockenmuller, B.W. Messmore, C.J. Hawker, Development of Thermal and Photochemical Strategies for Thiol−Ene Click Polymer Functionalization, Macromolecules 41(19) (2008) 7063-7070.
[58] S.P.S. Koo, M.M. Stamenović, R.A. Prasath, A.J. Inglis, F.E. Du Prez, C. Barner-Kowollik, W. Van Camp, T. Junker, Limitations of radical thiol-ene reactions for polymer–polymer conjugation, Journal of Polymer Science Part A: Polymer Chemistry 48(8) (2010) 1699-1713.
[59] J. Justynska, H. Schlaad, Modular Synthesis of Functional Block Copolymers, Macromolecular Rapid Communications 25(16) (2004) 1478-1481.
[60] T.M. Roper, C.A. Guymon, E.S. Jönsson, C.E. Hoyle, Influence of the alkene structure on the mechanism and kinetics of thiol–alkene photopolymerizations with real-time infrared spectroscopy, Journal of Polymer Science Part A: Polymer Chemistry 42(24) (2004) 6283-6298.
[61] J. Yan, R.J. Spontak, Toughening Poly(lactic acid) with Thermoplastic Elastomers Modified by Thiol–ene Click Chemistry, ACS Sustainable Chemistry & Engineering 7(12) (2019) 10830-10839.
[62] F. Shao, X.F. Ni, Z.Q. Shen, Preparation of amphiphilic graft copolymer with polyisoprene backbone by combination of anionic polymerization and "click" reaction, Chinese Chemical Letters 23(3) (2012) 347-350.
[63] N.B. Cramer, S.K. Reddy, A.K. O'Brien, C.N. Bowman, Thiol−Ene Photopolymerization Mechanism and Rate Limiting Step Changes for Various Vinyl Functional Group Chemistries, Macromolecules 36(21) (2003) 7964-7969.
[64] C.E. Hoyle, T.Y. Lee, T. Roper, Thiol–enes: Chemistry of the past with promise for the future, Journal of Polymer Science Part A: Polymer Chemistry 42(21) (2004) 5301-5338.
[65] D.E. Fagnani, J.L. Tami, G. Copley, M.N. Clemons, Y.D.Y.L. Getzler, A.J. McNeil, 100th Anniversary of Macromolecular Science Viewpoint: Redefining Sustainable Polymers, ACS Macro Letters 10(1) (2021) 41-53.
[66] U. Kalita, S. Samanta, S.L. Banerjee, N.C. Das, N.K. Singha, Biobased Thermoplastic Elastomer Based on an SMS Triblock Copolymer Prepared via RAFT Polymerization in Aqueous Medium, Macromolecules (2021).
[67] M.P. Luda, M. Guaita, O. Chiantore, Thermal degradation of polybutadiene, 2. Overall thermal behaviour of polymers with different microstructures, Die Makromolekulare Chemie 193(1) (1992) 113-121.
[68] K. McCreedy, H. Keskkula, Application of thermogravimetric analysis to the thermal decomposition of polybutadiene, Journal of Applied Polymer Science 22(4) (1978) 999-1005.
[69] R.A. Mantz, P.F. Jones, K.P. Chaffee, J.D. Lichtenhan, J.W. Gilman, I.M.K. Ismail, M.J. Burmeister, Thermolysis of Polyhedral Oligomeric Silsesquioxane (POSS) Macromers and POSS−Siloxane Copolymers, Chemistry of Materials 8(6) (1996) 1250-1259.
[70] I.C. McNeill, W.T.K. Stevenson, Thermal degradation of styrene-butadiene diblock copolymer: Part 2—Characteristics and mechanism of degradation of the copolymer, Polymer Degradation and Stability 10(4) (1985) 319-334.
[71] L. Zheng, R.M. Kasi, R.J. Farris, E.B. Coughlin, Synthesis and thermal properties of hybrid copolymers of syndiotactic polystyrene and polyhedral oligomeric silsesquioxane, Journal of Polymer Science Part A: Polymer Chemistry 40(7) (2002) 885-891.

[72] T.S. Haddad, J.D. Lichtenhan, Hybrid Organic−Inorganic Thermoplastics: Styryl-Based Polyhedral Oligomeric Silsesquioxane Polymers, Macromolecules 29(22) (1996) 7302-7304.
[73] S. Spoljaric, A. Genovese, R.A. Shanks, Novel elastomer-dumbbell functionalized POSS composites: Thermomechanical and Morphological Properties, Journal of Applied Polymer Science 123(1) (2012) 585-600.
[74] E. McMullin, H.T. Rebar, P.T. Mather, Biodegradable Thermoplastic Elastomers Incorporating POSS: Synthesis, Microstructure, and Mechanical Properties, Macromolecules 49(10) (2016) 3769-3779.
[75] J.M. Hutchinson, Determination of the glass transition temperature, Journal of Thermal Analysis and Calorimetry 98(3) (2009) 579.
[76] J. Rieger, The glass transition temperature Tg of polymers—Comparison of the values from differential thermal analysis (DTA, DSC) and dynamic mechanical measurements (torsion pendulum), Polymer Testing 20(2) (2001) 199-204.
[77] K.S. Lee, Y.-W. Chang, Thermal and mechanical properties of poly(ε-caprolactone)/polyhedral oligomeric silsesquioxane nanocomposites, Polymer International 62(1) (2013) 64-70.
[78] J.M. Yu, P. Dubois, R. Jérôme, Synthesis and Properties of Poly[isobornyl methacrylate (IBMA)-b-butadiene (BD)-b-IBMA] Copolymers: New Thermoplastic Elastomers of a Large Service Temperature Range, Macromolecules 29(23) (1996) 7316-7322.
[79] E. Penzel, J. Rieger, H.A. Schneider, The glass transition temperature of random copolymers: 1. Experimental data and the Gordon-Taylor equation, Polymer 38(2) (1997) 325-337.
[80] F.S. Bates, G.H. Fredrickson, Block copolymer thermodynamics: theory and experiment, Annual review of physical chemistry 41(1) (1990) 525-557.
[81] D.W.V. Krevelen, K.T. Nijenhuis, Properties of Polymers - Their Correlation with Chemical Structure; Their Numerical Estimation and Prediction from Additive Group Contributions (4th, Completely Revised Edition), Elsevier, 1976, pp. 213-216.
[82] B. Brüster, Y.-O. Adjoua, R. Dieden, P. Grysan, C.E. Federico, V. Berthé, F. Addiego, Plasticization of Polylactide with Myrcene and Limonene as Bio-Based Plasticizers: Conventional vs. Reactive Extrusion, Polymers 11(8) (2019).
[83] İ. Kaya, E. Özdemir, Thermodynamic interactions and characterisation of poly(isobornyl methacrylate) by inverse gas chromatography at various temperatures, Polymer 40(9) (1999) 2405-2410.
[84] M. Morton, J.E. McGrath, P.C. Juliano, Structure-property relationships for styrene-diene thermoplastic elastomers, Journal of Polymer Science Part C: Polymer Symposia 26(1) (1969) 99-115.